



High Strain Rate Deformation Modeling of a Polymer Matrix Composite

Part I—Matrix Constitutive Equations

Robert K. Goldberg
Lewis Research Center, Cleveland, Ohio

Donald C. Stouffer
University of Cincinnati, Cincinnati, Ohio

National Aeronautics and
Space Administration

Lewis Research Center

Acknowledgments

The authors would like to acknowledge Fiberite, Inc. for providing the material used for the experimental tests along with information and data on the material. The authors would also like to acknowledge Cincinnati Testing Laboratories, Inc., for conducting the low strain rate tensile experiments presented in this report. The University of Dayton Research Institute Impact Physics Lab is also acknowledged for conducting the high strain rate experiments discussed in this study.

Trade names or manufacturers' names are used in this report for identification only. This usage does not constitute an official endorsement, either expressed or implied, by the National Aeronautics and Space Administration.

Available from

NASA Center for Aerospace Information
7121 Standard Drive
Hanover, MD 21076
Price Code: A03

National Technical Information Service
5287 Port Royal Road
Springfield, VA 22100
Price Code: A03

High Strain Rate Deformation Modeling of a Polymer Matrix Composite: Part I-Matrix Constitutive Equations

Robert K. Goldberg
National Aeronautics and Space Administration
Lewis Research Center
Cleveland, Ohio 44135

and

Donald C. Stouffer
University of Cincinnati
Cincinnati, Ohio 45221

SUMMARY

Recently applications have exposed polymer matrix composite materials to very high strain rate loading conditions, requiring an ability to understand and predict the material behavior under these extreme conditions. In this first paper of a two part report, background information is presented, along with the constitutive equations which will be used to model the rate dependent nonlinear deformation response of the polymer matrix. Strain rate dependent inelastic constitutive models which were originally developed to model the viscoplastic deformation of metals have been adapted to model the nonlinear viscoelastic deformation of polymers. The modified equations were correlated by analyzing the tensile/compressive response of both 977-2 toughened epoxy matrix and PEEK thermoplastic matrix over a variety of strain rates. For the cases examined, the modified constitutive equations appear to do an adequate job of modeling the polymer deformation response. A second follow-up paper will describe the implementation of the polymer deformation model into a composite micromechanical model, to allow for the modeling of the nonlinear, rate dependent deformation response of polymer matrix composites.

LIST OF SYMBOLS

D_0	material constant representing maximum inelastic strain rate
E	elastic modulus of material
n	material constant representing rate dependence of material
q	material constant representing hardening rate of material
S_{ij}	deviatoric stress component
t	current time
Δt	current time increment
Z	scalar state variable
Z_0	material constant representing initial isotropic hardness of material

Z_1	material constant representing value of scalar state variable at saturation
ϵ	uniaxial strain
ϵ^I	uniaxial inelastic strain
ϵ_{ij}^I	inelastic strain component
ϵ_e^I	effective inelastic strain
ϵ_s^I	inelastic strain at saturation
$\dot{\epsilon}_o$	constant total applied strain rate
Ω	uniaxial back stress
Ω_{ij}	back stress component
Ω_m	material constant representing value of back stress at saturation
σ	uniaxial stress
σ_s	value of stress at saturation
•	quantities with dots above them represent rates

INTRODUCTION

NASA Lewis Research Center has an ongoing research program to develop new technologies to improve aircraft engine fan containment systems. The program contains a feasibility study to replace metallic containment systems with polymer matrix composite hardwall containment systems. In such an application, the composite would be loaded at strain rates up to several hundred per second. In designing a polymer matrix composite containment system, the ability to correctly model the constitutive and failure behavior of the composite under the high rate loading conditions present is of critical importance.

Experimental techniques to characterize the behavior of polymer matrix composites under low strain rate loading conditions have been well established for many years. Furthermore, numerous analytical methods have been developed to model the constitutive and failure behavior of composites under quasi-static loads. However, the analytical methods required to characterize and model the constitutive and failure behavior of polymer matrix composites under high strain rates are not nearly as well developed as is the case for materials under quasi-static loads. Furthermore, the effects of strain rate on the material properties and response is still an area of active investigation.

This paper, the first of a two part report, describes the adaptation of constitutive equations designed to model the viscoplastic deformation response of metals to the problem of modeling the inelastic, strain rate dependent response of a polymer. First, some general background, including a review of the literature, will be presented. In the background section of this report, previous investigations into characterizing and modeling the rate dependent response of polymers and polymer matrix composites will be described. Specifically, experimental tests designed to determine the rate dependence of the properties and response of a polymer matrix composite will be described. In addition, analytical methods which have been developed to represent the rate dependent response of both bulk polymers and polymer matrix composites will be discussed.

After the background section, the strain rate dependent, inelastic constitutive equations which were utilized to model the polymer matrix will be discussed. For the constitutive equations, techniques which were originally designed to represent the rate-dependent, viscoplastic response of metals have been adapted and modified to model the inelastic response of a polymer. A description of these methods, and how they were modified to analyze the tensile/compressive response of a polymer, will be given. Furthermore, the analytical procedure utilized to obtain material constants for two representative materials, Fiberite 977-2 toughened epoxy and PEEK thermoplastic, will be described. The experimental procedures which were utilized to obtain the material data will also be presented. The computational approach used to implement the equations will be discussed, and the stress-strain curves obtained by using the developed models will be presented. Conclusions on which of the presented constitutive models will be utilized in the remainder of the project will be given.

BACKGROUND

Strain Rate Effects on Material Properties

Several experimental studies have been performed with the goal of determining the effects of strain rate on the material properties and response of polymer matrix composite systems at high strain rate conditions. One such method of performing such studies involves using the split Hopkinson bar technique, which was utilized by researchers such as Harding and Welsh [1], Staab and Gilat [2] and Choe, Finch and Vinson [3]. The technique has been extensively utilized in characterizing metals at high strain rates [4]. The basic technique involves propelling a striker bar into a pressure bar. The pressure bar then transmits a compression stress wave which propagates through the specimen, sandwiched between the pressure bar and a transmission bar. Gages on the pressure and transmission bars are then utilized to compute the force and displacement in the specimen based on the wave propagation profiles.

Harding and Welsh [1] created a modified split Hopkinson bar apparatus to allow for the tensile testing of unidirectional graphite/epoxy composites at high strain rates. Tests were conducted at strain rates ranging from $5E-04$ /sec to 450 /sec on composites with a [0] fiber orientation. The stress-strain curves obtained were nearly linear until failure, and there was minimal change in the elastic modulus and fracture strength with strain rate. Since the response of a [0] composite is primarily fiber dominated, these results indicate that the graphite fibers have minimal strain rate dependence. Harding also conducted split Hopkinson bar tests on glass/epoxy and glass/polyester woven composites loaded with a punch loading condition [5]. For both types of materials tested, the study found that increasing the punch speed resulted in an increase in the maximum punch load present in the specimen, as well as an increase in the shear strength of the specimen.

Staab and Gilat [2] conducted tensile split Hopkinson bar tests and static tests on glass/epoxy composites over a strain rate range from $1\text{E-}04$ /sec to approximately 1000 /sec. Laminates with fiber orientations ranging from $[\pm 15]_s$ to $[\pm 75]_s$ were examined. For each of the laminate orientations considered, increasing the strain rate increased the initial modulus, maximum stress and failure strain. The difference between the static results and the high strain rate results increased significantly as the laminate orientation angle decreased. In compressive split Hopkinson bar tests that Choe, Finch and Vinson [5] conducted, the ultimate stress and modulus were found to increase with strain rate for unidirectional graphite/epoxy specimens. The ultimate stress also increased with strain rate for quasi-isotropic graphite/epoxy specimens.

Another type of test technique utilized to determine the response of polymer matrix composites at high strain rates involves subjecting the composite to explosive pressure pulse loadings. Such methods were utilized by Daniel, Hsiao and Cordes [6], Daniel, Hamilton and LaBedz [7] and Al-Salehi, Al-Hassani and Hinton [8]. Daniel, et. al. [6,7] utilized an expanding ring, where a thin composite ring is subject to an explosive pulse loading. In combination with static tests, the effects of strain rate on the longitudinal, transverse and shear properties of a unidirectional graphite/epoxy composite system were determined. The experiments were conducted using strain rates ranging from $1\text{E-}04$ /sec to 500 /sec. In the longitudinal direction, the modulus increased slightly, but the strength and failure strain showed almost no variation as the strain rate was increased. In the transverse direction, on the other hand, the modulus and strength increased sharply, and the failure strain showed a slight increase with higher strain rates. When the shear properties were examined, the modulus increased significantly, the strength increased a moderate amount, and the failure strain showed a slight decrease with increasing strain rate. Since the longitudinal properties of a unidirectional composite system are fiber dominated, the results obtained indicate that for a graphite/epoxy composite the properties of the carbon fiber do not vary significantly with strain rate (similar to what was found by Harding and Welsh [1]). However, since the transverse and shear properties are matrix dominated, the results indicate that the behavior of the epoxy matrix does vary significantly with strain rate, and drives the rate dependence of the composite. Utilizing similar testing techniques, Al-Salehi, et. al. [8] found that for a filament wound glass-epoxy tube, the burst strength and failure strain increased, while the elastic modulus displayed minimal variation, with higher strain rates.

The correlation between the strain rate dependence of the composite and the rate dependence of the matrix, particularly at high strain rates, for graphite/epoxy composites was further established by Groves, et. al [9]. In compression tests on a graphite/epoxy composite, the compression strength was found to increase with strain rate, with the increase being most pronounced at higher strain rates (on the order of 100-1000 /sec). To attempt to explain this behavior, tensile and compressive stress-strain curves were generated for the epoxy matrix over a variety of strain rates. For both tensile and compressive loadings, the modulus was found to increase with strain rate, with significant increases occurring at strain rates above 10 /sec. Furthermore, the compressive strength was found to increase steadily with strain rate, while the tensile strength was found to

increase dramatically at strain rates above 10 /sec. The results from these tests confirmed that strain rate had a significant effect on the properties of the epoxy matrix in a graphite/epoxy system.

The overall result from these experimental studies is that while the details may vary based on the type of fiber and fiber orientation angle used, the material properties and response of polymer matrix composites do vary with strain rate, particularly at high strain rate conditions. In particular, for graphite/epoxy systems, the strain rate dependence appears to be driven by the strain rate dependence of the polymer matrix, indicating that in modeling composites of this type, capturing the rate dependent response of the polymer matrix is of critical importance.

Polymer Constitutive Modeling

Polymers have long been known to have a rate-dependent constitutive response. Traditionally, for very small strain response, linear viscoelastic techniques have been used to model the rate dependent behavior on a phenomenological level [10]. In linear viscoelastic models, combinations of springs and dashpots in series and parallel may be used to capture the rate dependent behavior. When the strains are large enough that the response is no longer linear, nonlinear viscoelastic models have been developed. For example, in a model developed by Cessna and Sternstein [11], nonlinear dashpots are incorporated into the constitutive model. Empirical equations are also used to capture the rate dependent response, in which the yield stress is scaled as a function of strain rate [12].

A more sophisticated approach to polymer constitutive modeling takes a molecular approach. In this approach [13], it is assumed that the deformation of a polymer is due to the motion of molecular chains over potential energy barriers. The molecular flow is due to applied stress, and the internal viscosity is assumed to decrease with applied stress. The yield stress (the point where permanent deformation begins) is defined as the point where the internal viscosity decreases to the point where the applied strain rate is equal to the plastic strain rate. Internal stresses can also be defined [13,14], which represent the resistance to molecular flow which tends to drive the material back towards its original configuration. Another approach to polymer deformation assumes that the deformation is due to the unwinding of molecular kinks [15]. In both approaches, constitutive models have been developed [13-17] in which the deformation response is considered to be a function of parameters such as activation energy, activation volume, molecular radius, molecular angle of rotation, and thermal constants. Furthermore, the deformation is assumed to be a function of state variables which represent the resistance to molecular flow caused by a variety of mechanisms. The state variable values evolve with stress, inelastic strain and inelastic strain rate.

An alternative approach to the constitutive modeling of polymers is to utilize, either directly or with some modifications, viscoplastic constitutive equations which have been developed for metals. For example, Bordonaro [18] modified the Viscoplasticity Theory

Based on Overstress developed by Krempl [19]. In Bordonaro's model, the original theory was modified to attempt to account for phenomena encountered in the deformation of polymers that are not present in metals. For example, polymers behave differently from metals under conditions such as creep, relaxation, and unloading. Other authors, such as Valisetty and Teply [20] and Zhang and Moore [21], utilized techniques developed to model the deformation of metals directly with no modification. However, they primarily limited their study to analyzing the uniaxial tensile response of polymers and did not consider phenomena such as unloading, creep or relaxation.

The conclusion to be drawn from the work discussed above is that it is possible to analyze the rate dependent response of polymers by simulating the physical deformation mechanisms. Furthermore, the physical deformation mechanisms can be modeled by the use of state variables. This approach is very similar to what is used in viscoplastic constitutive equations which are utilized for metals. The work completed to date indicates that modeling techniques developed for metals can be adapted for use with polymers. However, appropriate modifications must be made to the equations and consideration must be given to the range of applicability of the model.

Composite Constitutive Modeling

Previous efforts to simulate the rate dependent response of polymer matrix composites at high strain rates have utilized both macroscopic and micromechanics approaches. In the macroscopic approach, the composite material is modeled as an anisotropic, homogenous material, without any attention being paid to the individual constituents. For example, Weeks and Sun [22] developed a macroscopic, rate-dependent constitutive model to analyze the nonlinear high strain rate response of thick composite laminates. Building upon previous work conducted by Yoon and Sun [23] and Gates and Sun [24], the inelastic behavior of a carbon fiber reinforced thermoplastic was simulated through the use of a quadratic plastic potential function. A scaling function was defined to model the variation of the response due to varying fiber orientation of a single ply. The finite element method was utilized to analyze a composite laminate, where a layer of elements was used to simulate a single ply. The rate dependence of the deformation response was captured by varying the material properties as a function of strain rate. This technique was later modified by Thiruppukuzhi and Sun [25] in order to directly incorporate the rate dependence of the material response into the constitutive model. A similar type of approach was utilized by Espinosa, Lu, Dwivedi and Zavattieri [26]. However, the finite element procedures utilized were specifically reformulated to account for the dynamic, large deformation response often seen in high strain rate impact problems.

Other approaches have been used to model the high strain rate response of polymer matrix composites on the macroscopic scale. For instance, O'Donoghue, et. al. [27] assumed an orthotropic, linear elastic deformation response, but reformulated the constitutive equations to separate out the hydrostatic and deviatoric stresses. This stress separation facilitated implementation of the technique into a transient dynamic finite element code. A simple approach developed by Tay, Ang and Shim [28] utilized an

empirical model which scaled the “dynamic” stresses (i.e. the stresses due to dynamic loading) as a function of strain rate.

Research has also been conducted in simulating the high strain rate deformation response of polymer matrix composites utilizing a micromechanics approach. In micromechanics, the effective properties and response of the composite are computed based on the properties and response of the individual constituents. For example, Espinosa, Emore and Xu [29] utilized a finite element approach in which the fibers and matrix were explicitly modeled in the finite element mesh. A molecular, state variable based polymer constitutive equation, similar to what was described in the previous section of this report, was utilized to model the inelastic, rate dependent deformation response of the polymer. Another approach that has been taken utilizes analytical methods which explicitly compute the effective properties of the composite based on the properties of the constituents. For instance, Clements, et. al. [30] utilized the Method of Cells developed by Aboudi [31] to account for the stress wave propagation at the constituent level seen in an impact problem. Aidun and Addessio [32] also utilized the Method of Cells to simulate a high strain rate impact problem. For their analysis, they developed a nonlinear elastic constitutive equation to model the response of the polymer matrix. In addition, they reformulated the micromechanics equations to separate out the hydrostatic and deviatoric stress components to facilitate implementation of the technique into a transient dynamic finite element code.

The overall conclusion from this review is that the high strain rate deformation response of composite materials can be modeled using a variety of methods. Furthermore, the nonlinear response of the composite can be accounted for within the constitutive equations. In macroscopic techniques, the nonlinearity and rate dependence of the deformation response are accounted for at the ply level. In micromechanical techniques, the rate dependence and nonlinearity of the polymer matrix is modeled at the constituent level. The homogenization techniques then compute the effective deformation response of the composite based on the response of the individual constituents.

MATRIX CONSTITUTIVE MODEL

State Variable Modeling Overview

As discussed in the previous section, the rate dependence of a polymer matrix composite loaded at high strain rates is primarily a function of the rate dependence of the matrix constituent. Furthermore, the stress-strain response of polymers is nonlinear at loads above one or two percent strain [10]. Consequently, a need exists for constitutive equations which capture the nonlinear, rate dependent deformation response of the matrix material.

It is possible to utilize constitutive equations for polymers which incorporate the deformation mechanisms of the material. For polymers, deformation is due to the motion of the molecular chains in the material [13]. At small deformation levels, prior to yield, there is also a resistance to the molecular flow. In constitutive models, a state variable approach can be utilized to model the mechanisms which cause material deformation [33]. In this type of approach, the specific changes in the local details of the material microstructure are not simulated. Alternatively, variables are defined which are meant to represent the average effects of the deformation mechanisms which are present. These variables can evolve as a function of external parameters such as the stress, inelastic strain, and the current value of the state variable. Furthermore, the inelastic strain rate can be defined to be a function of the state variables and external variables such as the current stress state.

The state variable approach to constitutive modeling has been fairly extensively utilized to model the inelastic deformation response of metals, which exhibit a viscoplastic response above about one-half of the melting temperature. An important characteristic of this approach is that there is no defined yield stress or onset of inelasticity [33]. Alternatively, inelastic strain is assumed to be present at all values of stress. The inelastic strain is just assumed to be very small compared to the elastic strain at low stress levels. When the inelastic strain evolves to a more significant level, the stress-strain curve will then begin to exhibit a nonlinear response. Furthermore, a single, unified variable is utilized to represent all inelastic strains. The effects of viscoelasticity, plasticity and creep are not separated out in this type of approach, but are combined into one unified variable.

There is some physical motivation to utilize state variable models which were developed for metals to simulate the nonlinear deformation response of polymers. For polymers, while the nonlinear deformation response is due to nonlinear viscoelasticity as opposed to viscoplasticity, a unified inelastic strain variable can still be utilized to simulate the nonlinear behavior. In addition, the “saturation stress” in metals and the “yield stress” in polymers (the point where the stress-strain curve becomes flat) are both defined as the stress level at which the inelastic strain rate equals the applied strain rate in constant strain rate tests [13, 33].

In metals, the inelastic strain rate is often modeled as being proportional to the difference between the deviatoric stress and “back stress” tensors. The back stress is a resistance to slip resulting from the interaction of dislocations under a shear stress with a barrier. As dislocations pile up at a barrier, atomic forces will cause additional dislocations approaching the barrier to be repelled. This repelling force is referred to as the back stress. The back stress is in the direction opposite to the local shear stress in uniaxial loading (and thus will be orientation dependent in three dimensional loading). The net stress producing slip or inelastic strain is the difference between the shear stress and the back stress [33]. An isotropic initial resistance to slip is also present in metals due to the presence of obstacles such as precipitates, grains and point defects. This initial resistance to slip is often referred to as a “drag stress”. In an alternative modeling

approach, the inelastic strain rate can be modeled as being proportional to a single scalar hardening variable which includes the effects of both the “back stress” and the “drag stress” [33]. Similar concepts have been used in the deformation modeling of polymers. Ward [13] discusses how creep strain and plastic strain can be defined as being proportional to the difference between the applied stress and an “internal stress”. The internal stress is defined as evolving with increasing strain. Alternatively, Qian and Liu [17] define a nonlinear viscoelastic strain which is proportional to a single isotropic state variable at small deformation levels. In this case, the state variable represents the resistance to deformation due to the interaction of the molecular chains. An orientation dependent back stress state variable is also defined for this model, but it is only utilized in the large deformation, post-yield regime.

It is important to note several significant limitations in using models developed for metals to simulate the nonlinear deformation response of polymers. Polymers exhibit nonlinear strain recovery on unloading, while metals display linear elastic strain recovery. The unloading behavior of polymers may not be represented accurately with a constitutive equation which was developed for modeling metals. Furthermore, phenomena such as creep, relaxation and high cycle fatigue may not be simulated correctly in polymers with a metals based constitutive model. However, for predicting failure in high velocity impact loading, none of these phenomena are considered to be extremely significant. Specifically, for the application under consideration only tensile or compressive loading, along with at most one unloading cycle, will be considered.

The constitutive models considered will most likely only be valid for relatively ductile polymers such as thermoplastics or toughened epoxies, where the correlation between the polymer deformation response and the deformation response of metals is strongest. State variable type techniques have been used to model both amorphous and semi-crystalline polymers, and it is not clear at this time whether the degree of crystallinity in the polymer will have a significant effect on the applicability of the equations. To fully simulate the complete range of polymer deformation response, a combined viscoelastic-viscoplastic model would most likely be required. A combined viscoelastic-viscoplastic model would have the ability to completely represent all of the mechanisms present in polymer deformation. Efforts have been made by several researchers to develop such a model [16,17,34]. However, such a combined model, which could be very complex, will not be considered here in this preliminary study.

Constitutive Equation Overview

For this work, three constitutive equations were considered to simulate the deformation behavior of the polymer matrix. To determine which equation would provide the best representation of the material behavior, uniaxial stress-strain curves obtained at constant strain rate were characterized and modeled. For now, only the uniaxial simplifications of the equations are considered. An important point to note is that all of the equations in their three-dimensional formulation are based on deviatoric stresses and stress invariants, which for both polymers and metals are the primary causes

of inelastic deformation [12, 33]. In addition, only the equations for the inelastic strain rate are presented. However, for all of the equations the total strain rate should be considered to be the sum of the elastic strain rate and the inelastic strain rate, as follows for uniaxial loading:

$$\dot{\epsilon} = \frac{\dot{\sigma}}{E} + \dot{\epsilon}' \quad (1)$$

where $\dot{\epsilon}$ is the total strain rate, $\dot{\sigma}$ is the stress rate, $\dot{\epsilon}'$ is the inelastic strain rate, and E is the elastic modulus of the material.

Several key assumptions were made in all of the constitutive equations. First, even though in high strain rate impact situations adiabatic heating may be a significant issue, for this preliminary study temperature effects have been neglected, and all of the results were obtained for room temperature. Second, small strain conditions have been assumed. In reality polymers, particularly in compression, can be subject to very large strains. Furthermore, in high strain rate impact situations structures are subject to large deformations and rotations. However, incorporating large deformation and rotation effects into the constitutive equations would add a level of complexity which is beyond the scope of this study. For the purposes of this preliminary modeling effort, therefore, all large deformation effects have been neglected. Future efforts will include modifying the constitutive equations to account for large deformation effects. Finally, stress wave effects due to dynamic loading may play a significant role in the material response when subjected to high rate loading, even at the local constituent level [30]. For the purposes of this study, any stress wave effects will be assumed to be fully accounted for on the macroscopic level by a finite element code within which the model is implemented.

The first constitutive equation which was considered is a simple power law. This equation, based on an equation developed by Qian and Liu [17], bears a strong resemblance to the Maxwell equation, which is commonly used for linear viscoelastic analysis of polymers [10]. The model also bears a resemblance to an Arrhenius equation for dislocation creep in metals [33]. The inelastic strain rate has the following format, where a scale factor of 1 /sec is assumed to premultiply the right hand side of the equation to ensure dimensional compatibility.

$$\dot{\epsilon}' = \left(\frac{|\sigma|}{Z} \right)^n * \frac{\sigma}{|\sigma|} \quad (2)$$

In the equation $\dot{\epsilon}'$ is the inelastic strain rate, σ is the total stress, n is a material constant which controls the rate dependence of the deformation response, and Z is a scalar state variable which represents the resistance to molecular flow.

The evolution of the state variable Z can be defined using the following expression. The equation is the one used by Stouffer [33] to model the evolution of the scalar drag stress in metals. However, the inelastic strain rate is used instead of the inelastic work rate (as suggested by Walker [35]).

$$\dot{Z} = q(Z_1 - Z)|\dot{\epsilon}'| \quad (3)$$

In the equation \dot{Z} is the state variable rate, $\dot{\epsilon}'$ is the inelastic strain rate, and Z is the current value of the state variable. Material constants include q , which is the “hardening” rate, and Z_1 , which is the value of Z at saturation.

Equation (3) can be integrated to obtain the following form for the value of the state variable Z :

$$Z = Z_1 - (Z_1 - Z_0) \exp(-q|\epsilon'|) \quad (4)$$

where Z_0 (a material constant) is the initial value of Z , ϵ' is the inelastic strain, and all other terms are as defined for Equation (3).

The next constitutive equation which was considered is the expression developed by Bodner [36], which was originally utilized to model metals. This equation defines the inelastic strain rate as being proportional to the exponential of the stress. This type of relationship is somewhat similar in form to the molecular based constitutive models for polymers discussed by Ward [13]. Specifically, the inelastic strain rate is defined by the following equation:

$$\dot{\epsilon}' = \frac{2}{\sqrt{3}} D_0 \exp\left[-\frac{1}{2}\left(\frac{Z}{|\sigma|}\right)^{2n}\right] * \frac{\sigma}{|\sigma|} \quad (5)$$

where $\dot{\epsilon}'$ is the inelastic strain rate, σ is the stress, and Z is a scalar state variable which represents the resistance to molecular flow. Material constants include D_0 , which is a scale factor which represents the maximum inelastic strain rate, and n , which is a variable which controls the rate dependence of the deformation response. Equation (3) is once again used to specify the evolution of the state variable Z . This evolution law is slightly different from the equation utilized by Bodner in that the inelastic strain rate is used instead of the inelastic work rate.

The third model which was considered is the constitutive equation which was developed by Ramaswamy and Stouffer [33], which also was originally developed for metals. The major difference between the Bodner model and the Ramaswamy-Stouffer model is that the Stouffer model utilizes a tensorial state variable as opposed to a scalar state variable. The tensorial state variable represents an “internal stress” which models the resistance to molecular flow. This “internal stress” is similar to the “back stress”

concept utilized in metals, as discussed in the previous section. The inelastic strain rate is considered to be related to the difference between the applied stress and the internal stress. Unlike the scalar state variable utilized in the other two constitutive equations, the tensorial state variable is orientation dependent. The state variable is assumed to be equal to zero when the material is in its virgin state, and evolves towards a maximum value at saturation. By using this approach, as will be discussed later it is possible to model to some extent the nonlinear strain recovery observed during unloading for many polymers.

The inelastic strain rate is defined by the following equation:

$$\dot{\epsilon}' = \frac{2}{\sqrt{3}} D_0 \exp \left[-\frac{1}{2} \left(\frac{Z_0}{|\sigma - \Omega|} \right)^{2n} \right] * \frac{\sigma - \Omega}{|\sigma - \Omega|} \quad (6)$$

where $\dot{\epsilon}'$ is the inelastic strain rate, σ is the stress, and Ω is the state variable (called “back stress” in metals) which represents the resistance to molecular flow. Material constants include D_0 , which is a scale factor which represents the maximum inelastic strain rate, n , which is a variable which controls the rate dependence of the deformation response, and Z_0 , which represents the isotropic, initial “hardness” of the material before any load is applied. The value of the state variable Ω is assumed to be zero at the start of loading. While not apparent from the uniaxial form of the flow equation, Ω is a tensorial, not a scalar, variable.

The evolution of the state variable Ω is described by the following expression,

$$\dot{\Omega} = q\Omega_m \dot{\epsilon}' - q\Omega |\dot{\epsilon}'| \quad (7)$$

where $\dot{\Omega}$ is the state variable rate, $\dot{\epsilon}'$ is the inelastic strain rate, and Ω is the current value of the state variable. Material constants include q , which is the “hardening” rate, and Ω_m , which is the maximum value of the “back stress” at saturation. This equation is slightly different than the original equation developed by Ramaswamy and Stouffer [33], in that the original equation includes an additional stress rate term which is not used here. The original stress rate term was included in order to provide for additional hardening at low stress levels [33]. This additional hardening was found to not be required for the materials analyzed in this study. For tensile loading, where the absolute value of the inelastic strain rate equals the inelastic strain rate, Equation (7) can be integrated to obtain the following form:

$$\Omega = \Omega_m - \Omega_m \exp(-q\epsilon') \quad (8)$$

where ϵ' is the inelastic strain, and all other parameters are as defined for Equation (7). Note that in this uniaxial form, Equation (8) strongly resembles Equation (4). The only difference, the lack of a term representing the initial value of the state variable Ω in Equation (8), is related to the fact that this initial value is always zero.

Material Constant Determination

The procedure for determining the constants for the Ramaswamy-Stouffer model will be described here. The techniques for determining the material constants for the other two models are similar. Detailed discussions of the methods for finding the material constants can be found in [34,36,37]. D_0 is currently assumed to be equal to a value 10^4 times the maximum applied total strain rate, and is assumed to be the limiting value of the inelastic strain rate. Future investigations may be conducted to investigate whether a relationship between D_0 and the shear wave speed can be determined. Such a relationship could allow the effects of stress waves to be more completely accounted for within the matrix constitutive equations.

To determine n , Z_0 and Ω_m , the following procedure is utilized. First, the natural logarithm of both sides of Equation (6) is taken. The values of the inelastic strain rate, stress, and state variable Ω at “saturation” are substituted into the resulting expression. As a reminder, the “saturation stress” in metals (the point where the stress-strain curve becomes flat) is defined as the stress level at which the inelastic strain rate equals the applied strain rate in constant strain rate tensile tests [33]. As mentioned before, the “yield stress” in polymers has a similar definition [13], and is actually the mechanism which is being considered here. However, in order to maintain consistent terminology with the original development of the equations, the terms saturation and saturation stress will be used in this report. The equation which is obtained is as follows:

$$\ln \left[-2 \ln \left(\frac{\sqrt{3} \dot{\epsilon}_0}{2 D_0} \right) \right] = 2n \ln(Z_0) - 2n \ln(\sigma_s - \Omega_m) \quad (9)$$

where σ_s equals the “saturation” stress, $\dot{\epsilon}_0$ is the constant applied total strain rate, and the remaining terms are as defined in Equations (6) and (7).

To determine the required constants, a family of tensile (or compressive) curves obtained from constant strain rate tests are utilized, with each curve being obtained at a different strain rate. Data pairs of the total strain rate and saturation stress values from each curve are taken. Values for Ω_m are estimated for the material, with initial estimates ranging from 50% to 75% of the highest saturation stress found to work well. These estimates are similar to the values used for large-grain metals. For each strain rate, the natural logarithm of the difference between the value of the saturation stress level and the estimate for Ω_m is taken. This value is considered to be the x-coordinate of a point on a master curve. Likewise, for each strain rate the total strain rate value is substituted into the left hand side of Equation (9), and the computed value is considered to be the y-coordinate of a point on a master curve. The data pair obtained from the tensile curve at one strain rate thus represents one point on the master curve. The number of points in the master curve equals the number of strain rates at which tensile tests were conducted.

A least squares regression analysis can then be performed on the master curve. As suggested by Equation (9), the slope of the best fit line is equal to $-2*n$. The intercept of the best fit line is equal to $2*n*\ln(Z_o)$. The value for Ω_m can then be adjusted until an optimal fit to the data is obtained.

To determine the value for m , Equation (8) is utilized. At saturation, the value of the back stress is assumed to approach the maximum value, resulting in the exponential term approaching zero. Assuming that saturation occurs when the following condition is satisfied:

$$\exp(-q\epsilon_s^I) = 0.01 \quad (10)$$

the equation can be solved for q , where ϵ_s^I is the inelastic strain at saturation. The value of the inelastic strain at saturation is estimated by determining the total strain at saturation from a constant strain rate tensile curve, and subtracting the elastic strain from this value. The elastic strain at saturation is computed by dividing the saturation stress by the elastic modulus, as suggested by Equation (1). The value of the inelastic strain at saturation is substituted into Equation (10), and solved for q . If the inelastic strain at saturation is found to vary with strain rate, the parameter q must be computed at each strain rate and regression techniques utilized to determine an expression for the variation of q . Note that if compressive data is being characterized, the absolute value of the inelastic strain at saturation is to be utilized.

An important point to note is that the meaning and ranges of the material constants when the equations are used to model polymer deformation are not the same as when the equations are utilized for simulating the deformation of metals. For example, when analyzing metals using the Ramaswamy-Stouffer model, a value of n greater than or equal to 3.0 indicates that the response is relatively rate insensitive [33]. However, in modeling polymers, this rule of thumb most likely does not apply due to the differences in deformation mechanisms between the two types of materials. Furthermore, the rate dependence observed in polymers is not as dramatic as the rate dependence seen in metals. Similarly, other rules of thumb observed in analyzing the deformation response of metals most likely do not apply in modeling polymer deformation.

Three Dimensional Extension of Constitutive Equations

While the unidirectional representation for the Ramaswamy-Stouffer equations is described by Equations (6) and (7), the full three dimensional formulation for the flow equation, as described in [33], is as follows:

$$\dot{\epsilon}_{ij}^I = D_o \exp \left[-\frac{1}{2} \left(\frac{Z_o^2}{3K_2} \right)^n \right] * \frac{S_{ij} - \Omega_{ij}}{\sqrt{K_2}} \quad (11)$$

where S_{ij} is the deviatoric stress component, Ω_{ij} is the component of the state variable, $\dot{\epsilon}_{ij}^I$ is the component of inelastic strain, n and Z_0 are as defined in Equation (6), and K_2 is defined as follows:

$$K_2 = \frac{1}{2} (S_{ij} - \Omega_{ij}) (S_{ij} - \Omega_{ij}) \quad (12)$$

The back stress variable rate, $\dot{\Omega}_{ij}$, is defined by the following relation:

$$\dot{\Omega}_{ij} = \frac{2}{3} q \Omega_m \dot{\epsilon}_{ij} - q \Omega_{ij} \dot{\epsilon}_e^I \quad (13)$$

where $\dot{\epsilon}_e^I$ is the effective inelastic strain rate, defined as follows:

$$\dot{\epsilon}_e^I = \sqrt{\frac{2}{3} \dot{\epsilon}_{ij}^I \dot{\epsilon}_{ij}^I} \quad (14)$$

where repeated indices indicated summation using the standard indicial notation definitions [33]. The remainder of the terms are as defined in Equations (6) and (7).

A key difference between the three dimensional Ramaswamy-Stouffer equations, and other equations that use tensorial state variables, such as the Walker model [35], lies in the definition of the tensorial state variable. In the Ramaswamy-Stouffer model, the back stress is defined in the same manner as the stress deviator. Under uniaxial loading, the tensorial state variable tensor has the following format:

$$[\Omega_{ij}] = \begin{bmatrix} \frac{2}{3}\Omega & 0 & 0 \\ 0 & -\frac{1}{3}\Omega & 0 \\ 0 & 0 & -\frac{1}{3}\Omega \end{bmatrix} \quad (15)$$

where Ω represents the uniaxial value of the state variable. In the Walker model, the state variable tensor under uniaxial loading is defined as follows. This definition is similar to the definition of the plastic strain tensor in standard plasticity theory [33]:

$$[\Omega_{ij}] = \begin{bmatrix} \Omega & 0 & 0 \\ 0 & -\frac{1}{2}\Omega & 0 \\ 0 & 0 & -\frac{1}{2}\Omega \end{bmatrix} \quad (16)$$

While both tensors are deviatoric tensors, the varying definition of the state variable results in varying definitions of the K_2 term. Using the definition of Ω_{ij} specified in Equation (16), K_2 would be defined as follows:

$$K_2 = \frac{2}{3} \left(\frac{3}{2} S_{ij} - \Omega_{ij} \right) \left(\frac{3}{2} S_{ij} - \Omega_{ij} \right) \quad (17)$$

which is what is seen in the Walker equation.

As discussed by Stouffer and Dame [33], the values of the material constants for the full three dimensional formulation of the equations would be identical to those obtained using the uniaxial representation of the equations. Three dimensional formulations of the flow equation for the power law and Bodner models would be obtained in a similar manner. Since the state variable for the power law and Bodner model is a scalar variable, the evolution equation would not change from the uniaxial expressions except for replacing the uniaxial inelastic strain rate with the effective inelastic strain rate.

Numerical Implementation of Ramaswamy-Stouffer Model

To implement the constitutive equations into a computer code, the following algorithm was utilized, shown pictorially as a flow chart in Figure 1. The same basic algorithm was utilized for all three constitutive models, and closely follows the procedure described in [33]. For initial verification, the uniaxial representation of the models was utilized. However, the results obtained using the uniaxial representation of the modified Ramaswamy-Stouffer equations were compared to results obtained using the full three dimensional formulation, and the results were identical. The computer code assumed strain controlled loading, since when implemented into a finite element code as a user defined material model subroutine strains would be supplied as the input. An iterative procedure is used, and for each time step the iteration loop is entered knowing the strain at time $t+\Delta t$, and knowing the stress and the values of all of the state variables (and their rates) at time t . The goal of the iterative procedure is to compute the stresses and the values of the state variables (and their rates) at time $t+\Delta t$. An implicit trapezoidal rule integration procedure with a constant time step was utilized. Although not described here, an explicit Runge-Kutta integration procedure was also developed and tested, yielding results identical to the implicit integrator. For the stand alone computer codes, implicit integration techniques are preferable to use due to their numerical stability [38]. However, when these equations are eventually implemented into transient dynamic finite element codes, the use of explicit integration techniques for the material model might be required due to the structure of the finite element algorithms.

The detailed procedures for implementing the Ramaswamy-Stouffer model will be discussed in this section. Computations using the other constitutive equations would utilize similar techniques. First, the material constants and load history are read from an input file, and all appropriate variables are initialized. Upon entering the time step loop,

the strain rate and the value of any strain rate dependent material properties are computed, and the total strain at time $t+\Delta t$ is determined. The first time through the iteration loop, an estimate for the stress at time $t+\Delta t$ is computed using the following forward Euler estimate:

$$\sigma(t + \Delta t) = E[\varepsilon(t + \Delta t) - \varepsilon^I(t) - \dot{\varepsilon}^I(t)\Delta t] \quad (18)$$

In this equation and the following equations in this section, t represents the current time, Δt represents the time increment, and all other variables are as defined in Equation (1) and Equations (6)-(8). A forward Euler estimate for the back stress (tensorial state variable) rate and a trapezoidal rule estimate for the back stress at time $t+\Delta t$ are given by the following expressions:

$$\dot{\Omega}(t + \Delta t) = q\Omega_m \dot{\varepsilon}^I(t) - q[\Omega(t) + \dot{\Omega}(t)\Delta t]|\dot{\varepsilon}^I(t)| \quad (19)$$

$$\Omega(t + \Delta t) = \Omega(t) + \frac{\Delta t}{2}[\dot{\Omega}(t + \Delta t) + \dot{\Omega}(t)] \quad (20)$$

Once the back stress is computed, the inelastic strain rate and the accumulated inelastic strain at time $t+\Delta t$ can be computed using the following expressions:

$$\dot{\varepsilon}^I(t + \Delta t) = \frac{2}{\sqrt{3}} D_0 \exp \left[-\frac{1}{2} \left(\frac{Z_0}{|\sigma(t + \Delta t) - \Omega(t + \Delta t)|} \right)^{2n} \right] * \frac{\sigma(t + \Delta t) - \Omega(t + \Delta t)}{|\sigma(t + \Delta t) - \Omega(t + \Delta t)|} \quad (21)$$

$$\varepsilon^I(t + \Delta t) = \varepsilon^I(t) + \frac{\Delta t}{2}[\dot{\varepsilon}^I(t + \Delta t) + \dot{\varepsilon}^I(t)] \quad (22)$$

After the first time through the iteration loop, the stress estimate for time $t+\Delta t$ is computed using the following trapezoidal rule estimate, where the inelastic strain rate estimate for time $t+\Delta t$ comes from the previous iteration :

$$\sigma(t + \Delta t) = E[\varepsilon(t + \Delta t) - \varepsilon^I(t) - [\dot{\varepsilon}^I(t + \Delta t) + \dot{\varepsilon}^I(t)]\frac{\Delta t}{2}] \quad (23)$$

The back stress rate estimate is computed using the following expression, while the back stress estimate for time $t+\Delta t$ is computed using Equation (20):

$$\dot{\Omega}(t + \Delta t) = q\Omega_m \dot{\varepsilon}^I(t + \Delta t) - q[\dot{\Omega}(t + \Delta t)]|\dot{\varepsilon}^I(t + \Delta t)| \quad (24)$$

The inelastic strain rate and inelastic strain estimate for time $t+\Delta t$ are computed using Equations (21) and (22).

MODEL CORRELATIONS

High Strain Rate Compression Analyses: Fiberite 977-2

Two materials were considered for this study, Fiberite 977-2 and PEEK. Consider first Fiberite 977-2, a toughened epoxy. Since toughening the polymer makes it more ductile and more damage resistant [39] than traditional epoxy resins, a material of this type would be more likely to be used in applications where impact resistance is required. To obtain the data needed to characterize this material, a two stage testing program was carried out. First, high strain rate tensile tests were performed. This work was conducted by University of Dayton Research Institute Impact Physics Lab [40].

Compression tests under strain rates varying from approximately 500 /sec to 1500 /sec were conducted, in which the material was loaded at as close to constant strain rate as could be achieved, and then unloaded (at varying strain rates) at an arbitrary point. The split Hopkinson bar testing technique was utilized to obtain the data. Engineering stress and engineering strain were measured due to the small strain assumptions which were made for the model. Three experiments were conducted for each strain rate. All three tests at each strain rate yielded similar values, therefore only the stress-strain curves from one of the experiments at each strain rate will be shown in the results which follow. Stress-strain curves obtained at nominal strain rates of 500 /sec, 1000 /sec and 1500 /sec are shown in Figure 2. An important point to note is that although the stresses obtained are actually compressive, they are shown as positive values to promote ease of graph interpretation. As can be seen in the figure, there is a definite, although relatively small, rate dependence of the material response. As mentioned earlier, the rate dependence observed in polymer deformation is often much less than what is observed in the deformation of metals. Furthermore, the results were obtained over a relatively small strain rate range (a factor of three). One important point to note is that, although not shown here, there is considerable deformation beyond yield (or "saturation"), particularly at the higher strain rates. However, only the portions of the curve up until yield is reached were used to characterize the material models. Only a limited portion of the stress strain curve was used because, for the application under consideration, the compressive strain levels observed were not expected to approach or exceed the saturation strain. However, since the material models utilized rely heavily on the "saturation" stress and strain to obtain the material constants, the data up until saturation was utilized. In addition, although not shown here, the stress-strain curves displayed significant nonlinearity upon unloading.

High strain rate tensile tests were also conducted on the material, but the tests yielded unusual results which could not be appropriately explained. Specifically, the stress-strain curves exhibited a bi-linear response, with the secondary linear region having a lower slope than was seen in the tensile response at low strain rates, which contradicts what is normally expected in polymers [12]. Since these results could not be appropriately explained, at the current time the high strain rate tensile data will not be used.

Using the compressive curves obtained at high strain rates, the following inelastic constants were obtained for the Fiberite 977-2 material for high strain rate compression:

Power Law: $n=20$, $Z_0=104$ MPa, $Z_1=186$ MPa, $q=41$

Bodner: $D_0=1E+07$ /sec., $n=1.0$, $Z_0=317$ MPa, $Z_1=1070$ MPa, $q=41$

Stouffer: $D_0=1E+07$ /sec., $n=0.36$, $Z_0=5560$ MPa, $q=41$, $\Omega_m=170$ MPa

A constant Poisson's ratio of 0.40 was utilized. This value was obtained from low strain rate tensile data, and was assumed to be valid for high strain rate compression. The high strain rate compression modulus was found to have a slight variation with strain rate, with average values as follows:

<u>Strain Rate (/sec.)</u>	<u>Modulus (GPa)</u>
500	9.6
1000	10.8
1500	11.7

Compressive stress-strain curves computed using the power law, Bodner, and Ramaswamy-Stouffer constitutive equations, along with experimentally obtained results, are shown in Figures 3-5 for constant strain rates of 500 /sec, 1000 /sec, and 1500 /sec. As can be seen in the figures, for all three strain rates the stress levels computed by the power law model do not correlate well with the stress levels observed in the experimental results. However, the Bodner and Stouffer models compute nearly identical results, and correlate much more favorably with the experimental values. Specifically, the onset of nonlinearity, the "saturation" of the stress strain curve and the strain rate dependence are correlated reasonably well by these two models. The fact that the Bodner and Ramaswamy-Stouffer models yield similar results is not surprising, as the Ramaswamy-Stouffer model is based on the Bodner equations. The discrepancies between the experimental and computed results seen at the lower strain levels are most likely due to the nature of the experimental tests. Specifically, in a split Hopkinson bar experiment a certain amount of time is required for the specimen to achieve a constant strain rate. Furthermore, at low strain levels the measured strains are often not completely accurate. A combination of these factors most likely resulted in the shape of the experimental curves, and the variation between the experimental and computed results.

While the Bodner and Stouffer models compute very similar results, a significant difference between the two models can be seen in Figure 6, where a load/unload cycle was computed using the Stouffer model for a strain rate of 500/ sec. As can be seen in the figure, there are some elements of nonlinear strain recovery in the unloading curve, which would be expected in a polymer [10]. While the nonlinearity is most likely not as extensive as would be present in the actual polymer, the mechanism is at least accounted for to some extent. As mentioned earlier, incomplete modeling of the nonlinear strain recovery during unloading is a major deficiency in utilizing viscoplastic constitutive models developed for metals to model the nonlinear viscoelastic deformation present at small deformation levels in polymers. This deficiency could be overcome by modifying

the constitutive equations, or by combining viscoelastic and viscoplastic terms into one set of constitutive equations. One possible modification which might be investigated for the Ramaswamy-Stouffer model is to reintroduce the stress rate term into the state variable evolution law which was included in the original equations [33]. The stress rate term was not utilized in the equations utilized here. This term would promote a faster decrease in the value of the state variable during unloading (due to the negative stress rate), which might allow for more significant nonlinear strain recovery. However, any investigation of this type is beyond the scope of the preliminary investigative study presented here.

It is not possible to simulate nonlinear strain recovery during unloading using the Bodner model, as the state variable monotonically approaches a saturation value and remains constant, even during unloading. In the Ramaswamy-Stouffer model, on the other hand, by utilizing the difference between the deviatoric stress and the “back stress” in the inelastic strain rate equation, once the stress level decreases to a level below that of the current back stress, the inelastic strain rate can decrease while unloading takes place. Furthermore, as mentioned above, the structure of these equations lead themselves to possible future modifications which might promote improved simulation of the nonlinear strain recovery. These results indicate that the modified Ramaswamy-Stouffer is the optimal model to use as the polymer constitutive model for this study, and the remaining analyses will be conducted using this model.

Low Strain Rate Tension Analyses: Fiberite 977-2

To further investigate the selected material model, tensile tests at low strain rates, ranging from $1\text{E-}04$ /sec. to 0.1 /sec., were conducted on the Fiberite 977-2 material by Cincinnati Testing Labs, Inc. [41]. Although the application under consideration is a high strain rate application, these experiments were conducted in order to characterize the full range of material behavior of the Fiberite 977-2 epoxy. By obtaining data over a wide strain rate range, the material could be more completely characterized, and the rate dependence of the material response could be more completely examined. In addition, performing low strain rate tensile tests would permit the obtaining of tensile data in a manner which would avoid the problems encountered in conducting the high strain rate tensile tests. Axial testing was utilized to obtain the data. Once again, engineering stress and engineering strain were measured due to the small strain assumptions which were made. Stress-strain curves obtained at constant strain rates of 0.0001 /sec., 0.01 /sec. and 0.1 /sec. are shown in Figure 7. As can be seen in the figure, there is a definite rate dependence to the tensile response. It should be noted that the unusual response seen at low strain levels for the two higher strain rates is most likely due to difficulties which were encountered in ramping up to the desired strain rate during the experimental tests.

A unique set of material constants was obtained from the low strain rate tensile data. It was not deemed advisable to use the material constants which were obtained from the high strain rate compression tests to model the low strain rate tensile response. One reason for not using the high strain rate compression constants is that in polymers there

are often differences in the material response between tensile and compressive loading. First of all, the yield stress in polymers has been found to be a function of the hydrostatic stress [13], which can cause a difference in the tensile and compressive response. Furthermore, in tension polymers can be subject to the formation of crazes, which causes yielding at a much lower stress level than in situations where shear yielding is the primary yield mechanism [42]. In compression, polymers are only subject to shear yielding. Crazing can also lead to the formation of cracks, which results in the polymer having a more brittle response in tension, and a more ductile response in compression [42]. Even if the material behavior did not change significantly between tension and compression over major portions of the stress-strain curve, since the high strain rate compressive material constants were obtained over a relatively limited strain rate range, the constants obtained may not be valid over the entire range of strain rates.

To attempt to provide further information on the material behavior, which could then be utilized to more completely and accurately determine a unified set of material constants, compression tests at low strain rates are currently being conducted at the NASA Lewis Research Center. From this data, a more complete set of compressive material constants will be obtained. In addition, by comparing the low strain rate compression response to the low strain rate tensile response, attempts will be made to obtain a unified set of material constants covering both tensile and compressive behavior over the full range of strain rates. A unified set of material constants will be critical in actual applications, such as utilizing the constitutive model in a transient dynamic finite element analysis to model impact problems. Furthermore, the rate dependence of the material response can be more completely determined by obtaining a unified set of material constants. If the low strain rate compression data cannot be obtained, the high strain rate compression data and the low strain rate tensile data might be combined using a suitable set of approximations to obtain a unified set of material constants.

To obtain the low strain rate tensile material constants, the stress-strain curves had to be extrapolated since the tensile specimens failed before "saturation" occurred. To obtain an estimate of the saturation stress and strain, the curves for the strain rates of 0.0001 /sec and 0.1 /sec were extrapolated using a quadratic curve fit. Since the specimens failed in tension before the saturation level was reached, it was assumed that matching the actual saturation stress would not be critical. Once low strain rate compression data is obtained, this data will be used to refine the material constants. By extrapolating, the following estimates for saturation stress and saturation strain for the low strain rate tensile data were obtained:

<u>Strain Rate (/sec.)</u>	<u>Saturation Stress (MPa)</u>	<u>Saturation Strain</u>
1E-04	97	0.055
0.1	110	0.053

The low strain rate tensile material constants for the Ramaswamy-Stouffer model, which were determined using the procedure discussed previously, are as follows: $D_0=1E+04$ /sec., $n=0.50$, $Z_0=1030$ MPa, $q=160$, $\Omega_m=69$ MPa. The low strain rate tensile elastic modulus was found to be rate dependent as follows:

<u>Strain Rate (/sec.)</u>	<u>Modulus (GPa)</u>
1E-04	3.65
0.01	4.13
0.1	4.82

It should be noted that the low strain rate tensile modulus values are somewhat less than the high strain rate compressive modulus values. Assuming that the tensile and compressive moduli follow similar trends with strain rate, this modulus variation with strain rate is consistent with what has been observed in literature, as described in the background section of this report. A constant Poisson's ratio of 0.40 was once again utilized.

Tensile stress-strain curves were computed for constant strain rates of 0.0001/ sec, 0.01 /sec, and 0.1 /sec using the Ramaswamy-Stouffer constitutive equations and the low strain rate tensile material constants presented above, and the results are shown in Figures 8-10. As can be seen in the figures, the computed results correlate with the experimental values reasonably well overall. In particular, the nonlinearity of the stress-strain curves is correlated reasonably well for all three strain rates. Any discrepancies between the experimental and computed results is most likely due to the approximations which were made in estimating the saturation stress and strain. Since the constants used in the constitutive equations are strongly dependent on these values, any inaccuracies in these values could significantly affect the computed results. Furthermore, for the experiments conducted at strain rates of 0.01 /sec and 0.1 /sec, as mentioned earlier difficulties were encountered during the tests in ramping up to the desired strain rate, which could have affected the experimental results.

Low Strain Rate Tension Analyses: PEEK

To determine if the selected constitutive model can accurately compute the stress-strain behavior of a variety of materials, plus to verify the low strain rate tensile capabilities of the constitutive equations for a material which has a distinct "saturation" in the stress-strain tensile response, a PEEK (polyetheretherketone) thermoplastic was also characterized and modeled. Tensile stress strain curves over strain rates ranging from 1E-06 /sec. to 1E-03 /sec. were obtained by Bordonaro and Krempl [43]. As mentioned previously, the tensile curves for this material exhibit a distinct saturation, or flattening out, unlike the tensile curves for the Fiberite 977-2 epoxy. This result is to be expected since a thermoplastic like PEEK is expected to be more ductile than the toughened epoxy Fiberite 977-2. A constant elastic modulus of 4000 MPa and a constant Poisson's ratio of 0.40 were utilized. The inelastic constants for the Ramaswamy-Stouffer model were

determined using the procedures described earlier and are as follows: $D_0=1\text{E}+04$ /sec., $n=0.46$, $Z_0=630$ MPa, $q=310$, $\Omega_m=52$ MPa.

Tensile stress-strain curves were computed for constant strain rates of $1\text{E}-06$ /sec., $1\text{E}-04$ /sec. and $1\text{E}-03$ /sec. The computed curves and the corresponding experimental results are shown in Figures 11-13. As can be seen from the figures, the computed values correlate with the experimental results extremely well. Furthermore, the model appears to do a better job in simulating the response of the PEEK than it did in the simulations of the Fiberite 977-2 epoxy discussed above. The quality of the simulations for the PEEK is most likely due to the fact that the experimental tests yielded smooth stress-strain curves, with no obvious inconsistencies in the results. As discussed earlier, both the high strain rate compression curves and the low strain rate tension curves for the Fiberite 977-2 epoxy displayed inconsistencies in the measured stress-strain curves. Furthermore, since the measured stress-strain curves for PEEK displayed a distinct saturation, or flattening out, no extrapolations were required in order to obtain the material constants. These results indicate that if the polymer under consideration can be appropriately characterized, the constitutive equations can do a good job in computing the polymer response.

CONCLUSIONS

In this study, rate dependent, inelastic constitutive equations have been tested for two representative polymeric materials. The results presented here indicate that the Ramaswamy-Stouffer constitutive model can do a satisfactory job in computing the deformation response of a polymer. However, for the Fiberite 977-2 toughened epoxy, which will be the primary material utilized in future work on impact failure modeling and structural analysis using the finite element method, several areas of future work are indicated. Specifically, a unified set of material constants will be determined which will allow the modeling of both tensile and compressive behavior over a wide range of strain rates, with full incorporation of the complete rate dependence of the material response.

Several modifications may be made to the constitutive equations. First, efforts will be made to determine if a relationship between the D_0 material constant and the shear wave speed can be specified. Through such a relationship, the effects of the dynamic loading on the deformation response may be more accurately computed within the constitutive equations. A second modification may entail adding a stress rate term to the state variable evolution law. This modification may allow the nonlinear strain recovery during unloading to be more accurately computed. One other modification which might be made to the model is to develop a more mechanistically based method to capture the rate dependence of the elastic modulus. Currently, a simple curve fit is utilized.

In the second part of this two part report, the implementation of the matrix constitutive equations into composite micromechanical analysis techniques will be described. In this manner, the nonlinearities and rate dependence observed in the deformation response of carbon fiber reinforced composite plies subject to high strain rate loads can be predicted.

Furthermore, the nonlinearities observed in the composite response can be predicted based on the nonlinear response of the matrix constituent, which is the actual mechanism taking place.

Once the deformation model is completed, an impact failure model will be developed based on local failure mechanisms, and the combined deformation and failure model will be implemented into a transient dynamic finite element code. Full deformation and failure analyses will then be conducted on structures subject to impact loading conditions.

REFERENCES

1. Harding, J.; and Welsh, L.M.: A Tensile Testing Technique for Fiber Reinforced Composites at Impact Rates of Strain. *J. Mat. Sci.*, Vol. 18, pp. 1810-1826, 1983.
2. Staab, G.H.; and Gilat, A.: High Strain Rate Response of Angle-Ply Glass/Epoxy Laminates. *J. Comp. Mat.*, Vol. 29, pp. 1308-1320, 1995.
3. Choe, G.H.; Finch, W.W. Jr.; and Vinson, J.R.: Compression Testing of Composite Materials at High Strain Rates. Proceedings of the Fourth Japan-U.S. Conference on Composite Materials, Technomic Publishing Co., Lancaster, PA., pp. 82-91, 1988.
4. Nicholas, T.: Material Behavior at High Strain Rates. Impact Dynamics, J. Zukas; T. Nicholas; H. Swift; L. Greszczuk; and D. Curran, eds., Krieger Publishing Co., Malabar, FL., pp. 277-332, 1992.
5. Harding, J.: The High Speed Punching Behavior of Woven-Roving Glass-Reinforced Composites. Proceedings of the Conference on Mechanical Properties at High Rates of Strain, Inst. Phys. Conf. Ser. No. 47, Institute of Physics, Bristol, England, pp. 318-330, 1979.
6. Daniel, I.M.; Hsiao, H.M.; and Cordes, R.D.: Dynamic Response of Carbon/Epoxy Composites. High Strain Rate Effects on Polymer, Metal and Ceramic Matrix Composites and Other Advanced Materials, AD-Vol. 48, Y.D.S. Rajapakse and J.R. Vinson, eds., ASME, pp. 167-177, 1995.
7. Daniel, I.M.; Hamilton, W.G.; and LaBedz, R.H.: Strain Rate Characterization of Unidirectional Graphite/Epoxy Composite. Composite Materials: Testing and Design (Sixth Conference), ASTM STP 787, I.M. Daniel, ed., American Society of Testing and Materials, pp. 393-413, 1982.
8. Al-Salehi, F.A.R.; Al-Hassani, S.T.S.; and Hinton, M.J.: An Experimental Investigation into the Strength of Angle Ply GRP Tubes under High Rates of Loading. *J. Comp. Mat.*, Vol. 23, pp. 288-305, 1989.

9. Groves, S.E.; Sanchez, R.J.; Lyon, R.E.; and Brown, A.E.: High Strain Rate Effects for Composite Materials. Composite Materials: Testing and Design (Eleventh Volume), ASTM STP 1206, E.T. Camponeschi, Jr., ed., American Society of Testing and Materials, pp. 162-176, 1993.
10. Rosen, S.L.: Fundamental Principles of Polymer Materials. John Wiley and Sons, New York, 1982.
11. Cessna, L.C. Jr.; and Sternstein, S.S.: Viscoelasticity and Plasticity Considerations in the Fracture of Glasslike High Polymers. Fundamental Phenomena in the Material Sciences, 4, Fracture of Metals, Polymers and Glasses, L.J. Broutman, J.J. Duga, and J.J. Gilman, eds., Plenum Press, New York, pp. 45, 1967.
12. Miller, E.: Introduction to Plastics and Composites. Marcel Dekker, Inc., New York, 1996.
13. Ward, I.M.: Mechanical Properties of Solid Polymers. John Wiley and Sons, New York, 1983.
14. Amoedo, J.: Rate-Dependent Constitutive Equations and Process Modeling of Polymer Materials. PhD Dissertation, Rensselaer Polytechnic Institute, Troy, New York, 1990.
15. Boyce, M.C.; Parks, D.M.; and Argon, A.S.: Large Inelastic Deformation of Glassy Polymers. Part I: Rate Dependent Constitutive Model. Mechanics of Materials. Vol. 7, pp. 15-33, 1988.
16. Hasan, O.A.; and Boyce, M.C.: A Constitutive Model for the Nonlinear Viscoelastic Viscoplastic Behavior of Glassy Polymers. Poly. Eng. & Sci., Vol. 35, pp. 331-344, 1995.
17. Qian, Z. and Liu, S.: Unified Constitutive Modeling from Viscoelasticity and Viscoplasticity of Polymer Matrix Composites. Proceedings of the American Society of Composites Twelfth Technical Conference, R.F. Gibson and G.M. Newaz, eds., Technomic Publishing Co., Lancaster, PA, pp. 165-174, 1997.
18. Bordonaro, C.M.: Rate Dependent Mechanical Behavior of High Strength Plastics: Experiment and Modeling. PhD Dissertation, Rensselaer Polytechnic Institute, Troy, New York, 1995.
19. Krempl, E.; McMahon, J.J.; and Yao, D.: Viscoplasticity Based on Overstress with a Differential Growth Law for the Equilibrium Stress. Mech. Mat., Vol. 5, pp. 35, 1986.

20. Valisetty, R.R.; and Teply, J.L.: Overall Instantaneous Viscoplastic Properties of Composites. *J. Comp. Mat.*, Vol. 26, pp. 1708-1724, 1992.
21. Zhang, C.; and Moore, I.D.: Nonlinear Mechanical Response of High Density Polyethylene. Part II: Uniaxial Constitutive Model. *Poly. Eng. & Sci.*, Vol. 37, pp. 414-420, 1997.
22. Weeks, C.A.; and Sun, C.T.: Nonlinear Rate Dependence of Thick-Section Composite Laminates. High Strain Rate Effects on Polymer, Metal and Ceramic Matrix Composites and Other Advanced Materials, AD-Vol. 48, Y.D.S. Rajapakse and J.R. Vinson, eds., ASME, pp. 81-95, 1995.
23. Yoon, K.J.; and Sun, C.T.: Characterization of Elastic-Viscoplastic Properties of an AS4/PEEK Thermoplastic Composite. *J. Comp. Mat.*, Vol. 25, pp. 1277-1296, 1991.
24. Gates, T.S.; and Sun, C.T.: Elastic/Viscoplastic Constitutive Model for Fiber Reinforced Thermoplastic Composites. *AIAA Journal*, Vol. 29, pp. 457-463, 1991.
25. Thiruppukuzhi, S.V.; and Sun, C.T.: A Viscoplasticity Model for High Strain Rate Characterization of Polymeric Composites. Proceedings of the American Society of Composites Twelfth Technical Conference, R.F. Gibson and G.M. Newaz, eds., Technomic Publishing Co., Lancaster, PA, pp. 450-459, 1997.
26. Espinosa, H.D.; Lu, H.C.; Dwivedi, S.K.; and Zavattieri, P.D.: A Finite Deformation Anisotropic Plasticity Model for Fiber Reinforced Composites. Proceedings of the American Society of Composites Twelfth Technical Conference, R.F. Gibson and G.M. Newaz, eds., Technomic Publishing Co., Lancaster, PA, pp. 429-441, 1997.
27. O'Donoghue, P.E.; Anderson, C.E. Jr.; Friesenhahn, G.J.; and Parr, C.H.: A Constitutive Formulation for Anisotropic Materials Suitable for Wave Propagation Computer Programs. *J. Comp. Mat.*, Vol. 26, pp. 1860-1884, 1992.
28. Tay, T.E.; Ang, H.G.; and Shim, V.P.W.: An Empirical Strain Rate-Dependent Constitutive Relationship for Glass-Fibre Reinforced Epoxy and Pure Epoxy. *Composite Structures*, Vol. 33, pp. 201-210, 1995.
29. Espinosa, H.D.; Emore, G.; and Xu, Y.: High Strain Rate Behavior of Composites with Continuous Fibers. High Strain Rate Effects on Polymer, Metal and Ceramic Matrix Composites and Other Advanced Materials, AD-Vol. 48, Y.D.S. Rajapakse and J.R. Vinson, eds., ASME, pp. 7-18 1995.
30. Clements, B.E.; Johnson, J.N.; and Hixson, R.S.: Stress Waves in Composite Materials. *Physical Review E*, Vol. 54, pp. 6876-6888, 1996.
31. Aboudi, J.: Mechanics of Composite Materials: A Unified Micromechanical Approach. Elsevier, New York, 1991.

32. Aidun, J.R.; and Addessio, F.L.: An Enhanced Cell Model with Nonlinear Elasticity. *J. Comp. Mat*, Vol. 30, pp. 248-280, 1996.
33. Stouffer, D.C.; and Dame, L.T.: Inelastic Deformation of Metals. Models, Mechanical Properties and Metallurgy. John Wiley and Sons, New York, 1996.
34. Saleeb, A.F.; and Arnold, S.M.: A General Reversible Hereditary Constitutive Model: Part I-Theoretical Developments. NASA TM-107493, National Aeronautics and Space Administration, 1997.
35. Walker, K.P.: Research and Development Program for Nonlinear Structural Modeling with Advanced Time-Temperature Dependent Constitutive Relationships. NASA CR-165533, National Aeronautics and Space Administration, 1981.
36. Bodner, S.R.: Review of a Unified Elastic-Viscoplastic Theory. Unified Constitutive Equations for Creep and Plasticity, A.K. Miller, ed., Elsevier, Barking, Essex, England, 1987.
37. Stouffer, D.C.; and Bodner, S.R.: A Relationship Between Theory and Experiment for a State Variable Constitutive Equation. Mechanical Testing for Deformation Model Development, ASTM STP 765, R.W. Rohde and J.C. Swearingen, eds., American Society of Testing and Materials, pp. 239-250, 1982.
38. Kreyszig, E.: Advanced Engineering Mathematics, 7th Edition. John Wiley and Sons, New York, 1992.
39. Almen, G.R.; Byrens, R.M.; MacKenzie, P.D.; Maskell, R.K.; McGrail, P.T.; and Sefton, M.S.: 977 - A Family of New Toughened Epoxy Resins. 34th International SAMPE Symposium, pp. 259-270, 1989.
40. Sawas, O.: Compression and Tension Characterization of Neat Resin and Composite Systems at High Strain Rate. UDR-TR-97-157, University of Dayton Research Institute, Experimental and Applied Mechanics Group, 1997.
41. Gieseke, B.: Private Communication, Cincinnati Testing Laboratories, Inc., 1997.
42. Kinloch, A.J.; and Young, R.J.: Fracture Behavior of Polymers. Elsevier, Barking, Essex, England, 1983.
43. Bordonaro, C.M.; and Krempl, E.: The Rate-Dependent Mechanical Behavior of Plastics: A Comparison Between 6/6 Nylon, Polyetherimide and Polyetheretherketone. Use of Plastics and Plastic Composites: Materials and Mechanics Issues, MD-Vol. 46, V.K. Stokes, ed., ASME, pp. 43-56, 1993.

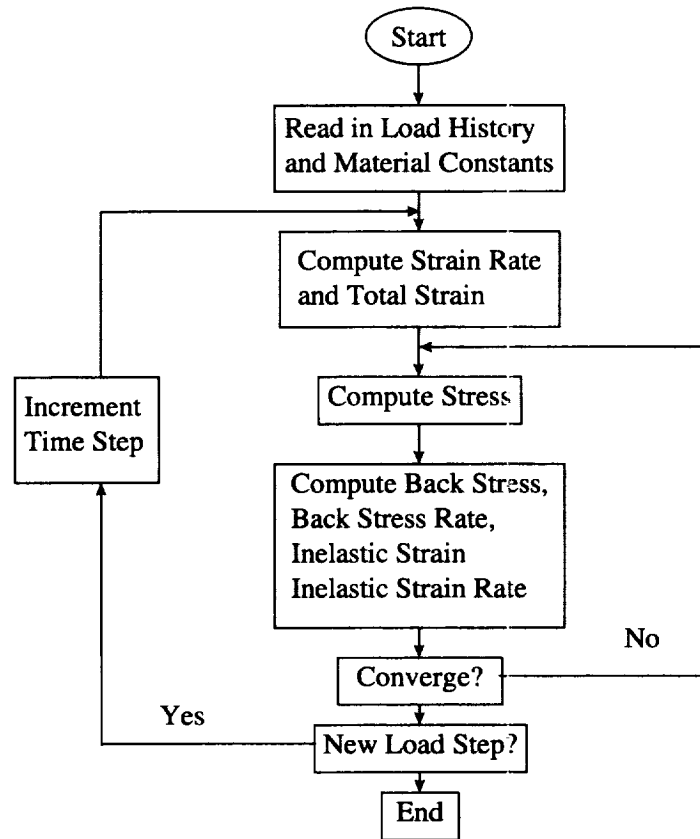


Figure 1: Flow Diagram for Matrix Constitutive Equation Algorithm

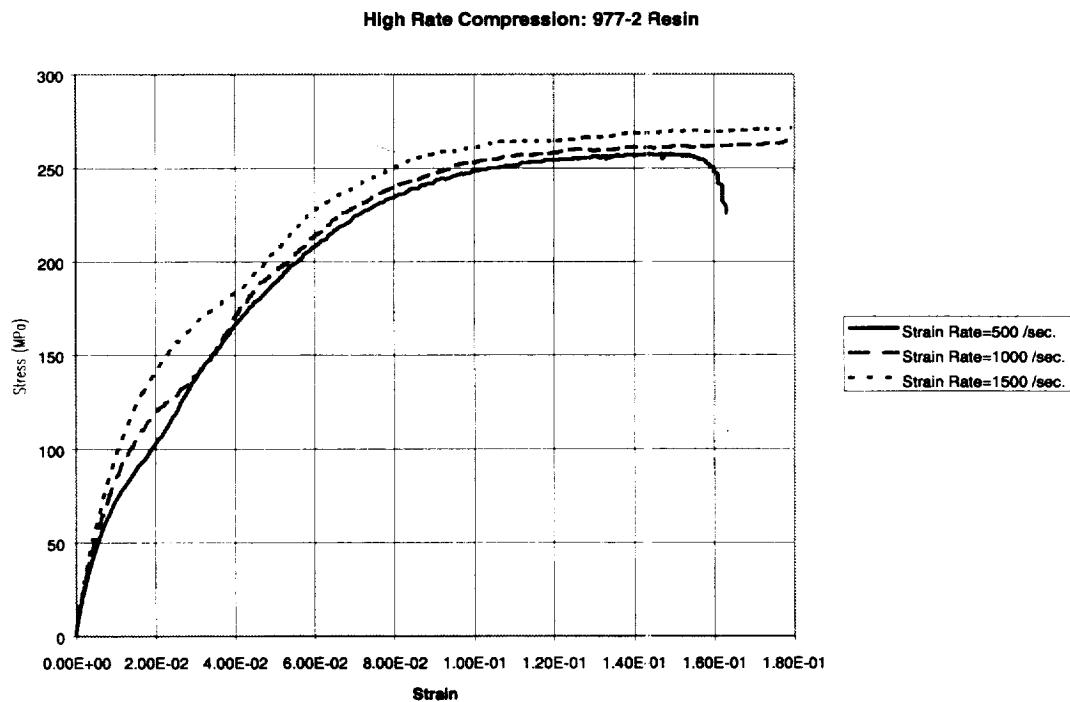


Figure 2: High Strain Rate Compression Curves for 977-2 Resin

High Rate Compression: 977-2 Resin, Strain Rate=500 /sec.

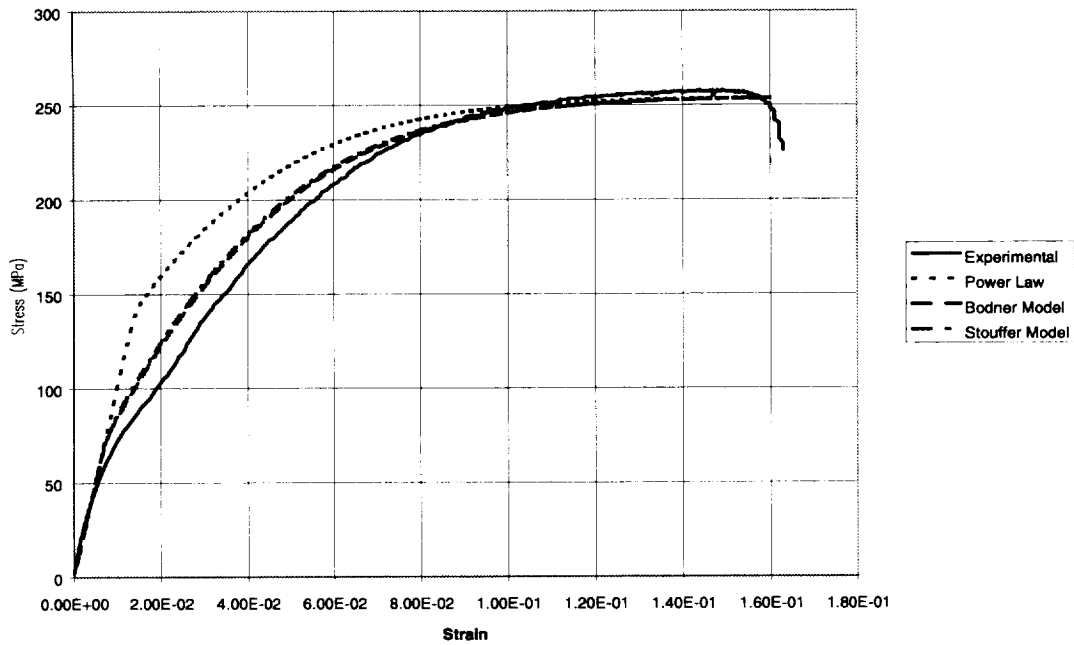


Figure 3: Model Correlations for 977-2 Resin at Compressive Strain Rate of 500 /sec.

High Rate Compression: 977-2 Resin, Strain Rate=1000 /sec.

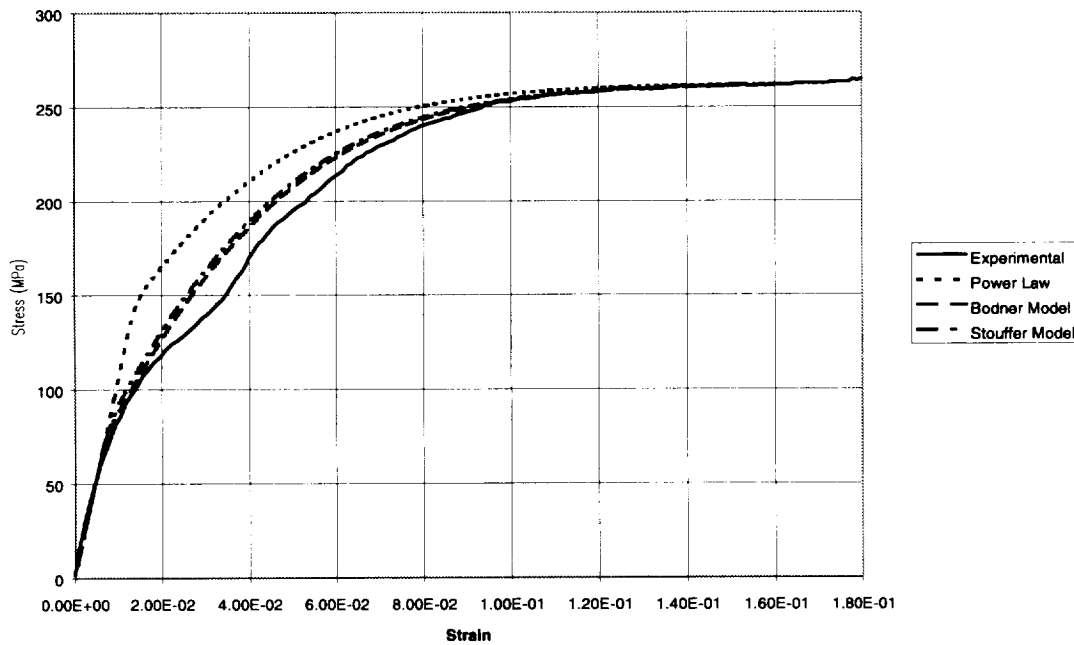
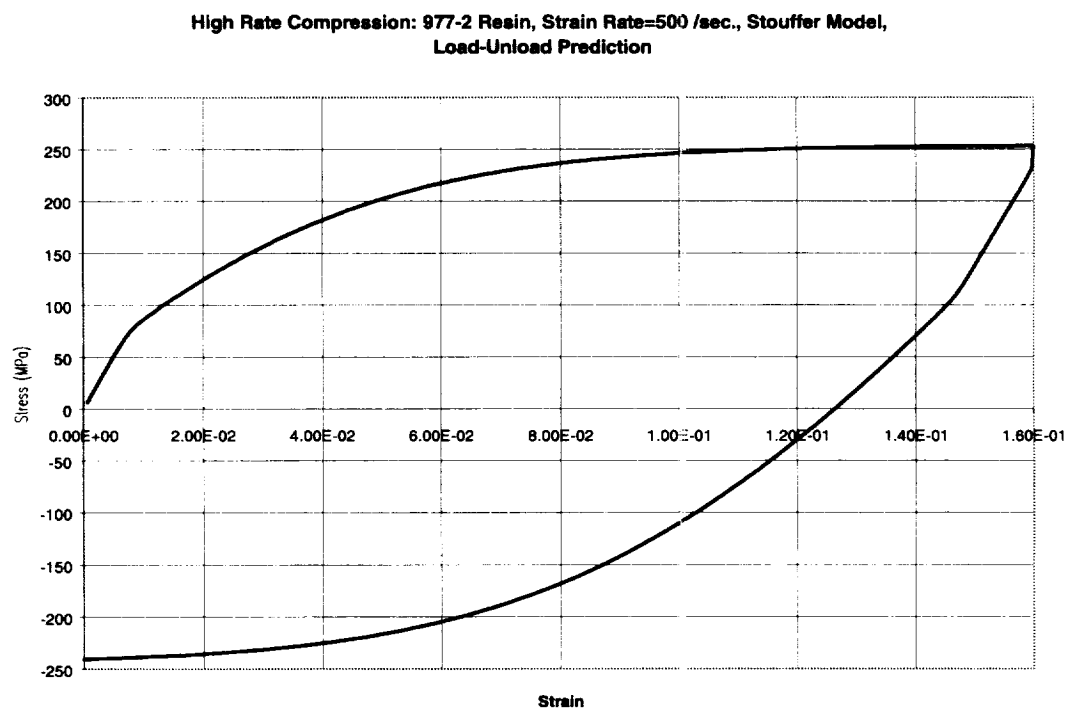
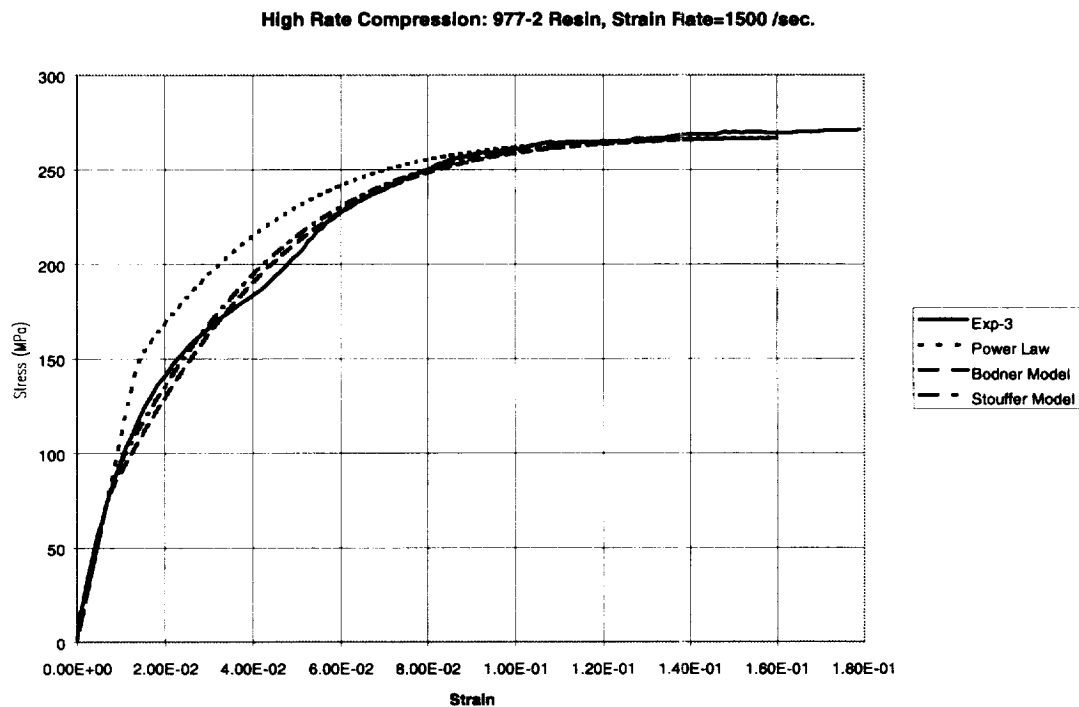


Figure 4: Model Correlations for 977-2 Resin at Compressive Strain Rate of 1000 /sec.



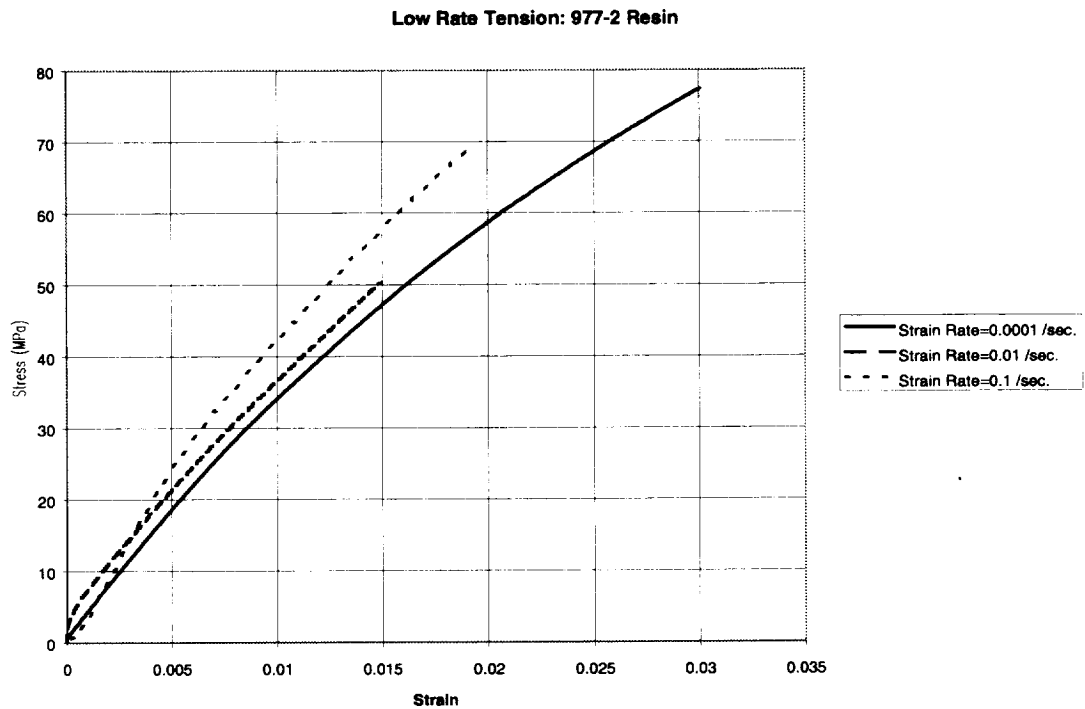


Figure 7: Low Strain Rate Tensile Curves for 977-2 Resin

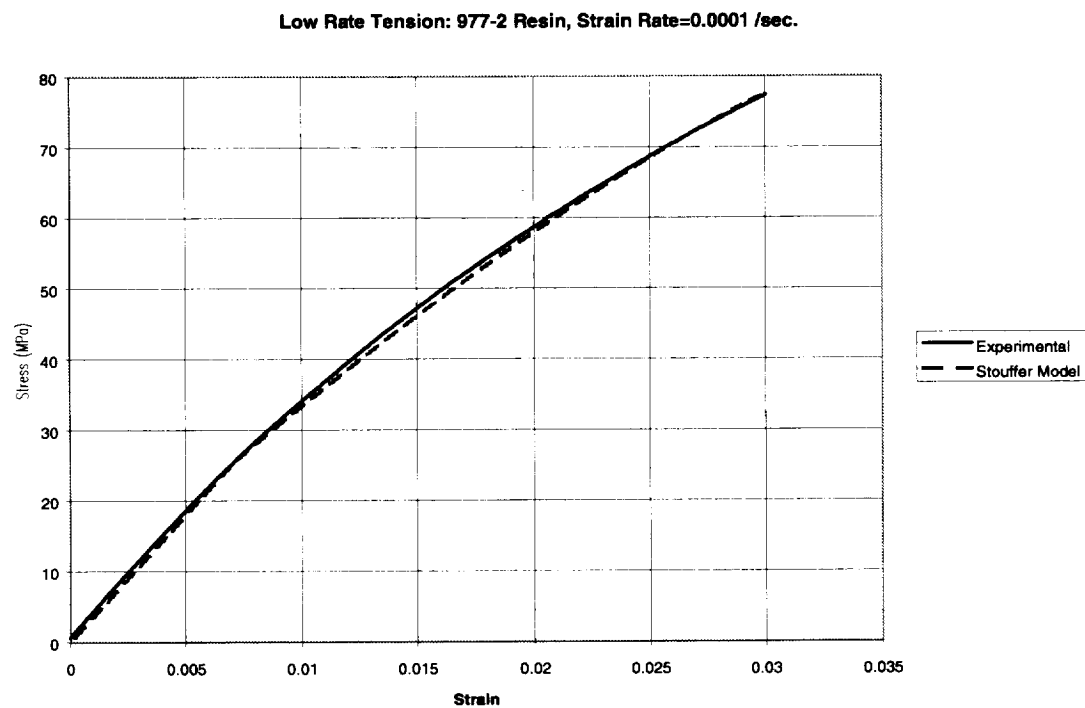


Figure 8: Model Correlations for 977-2 Resin at Tensile Strain Rate of 0.0001 /sec.

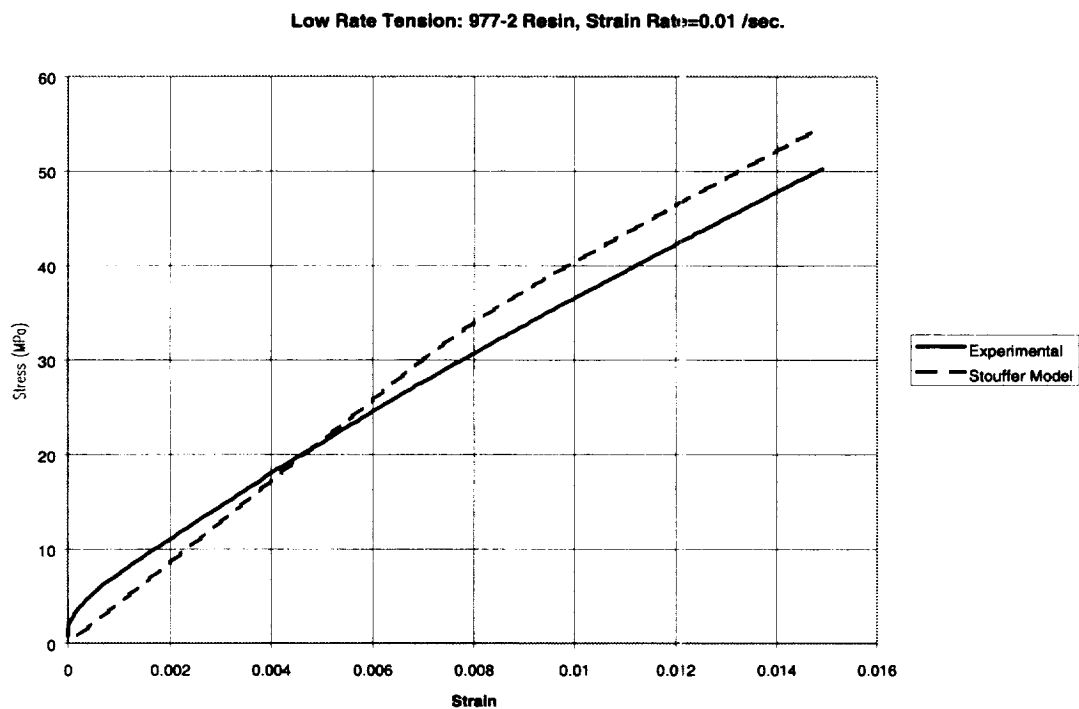


Figure 9: Model Correlations for 977-2 Resin at Tensile Strain Rate of 0.01 /sec.

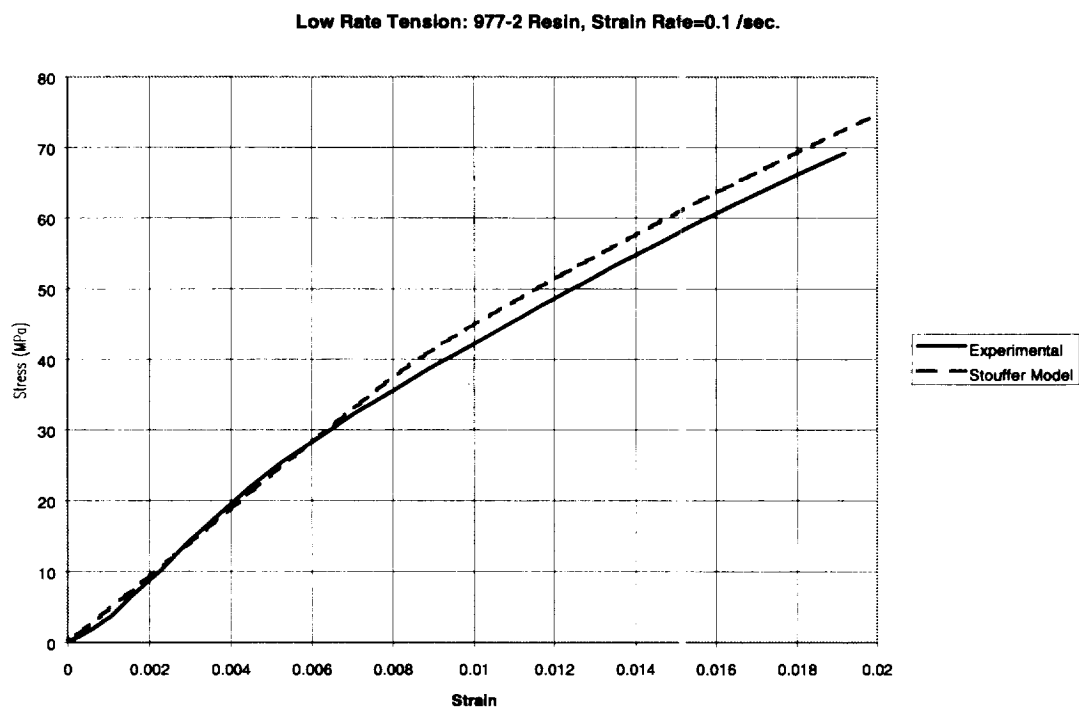


Figure 10: Model Correlations for 977-2 Resin at Tensile Strain Rate of 0.1 /sec.

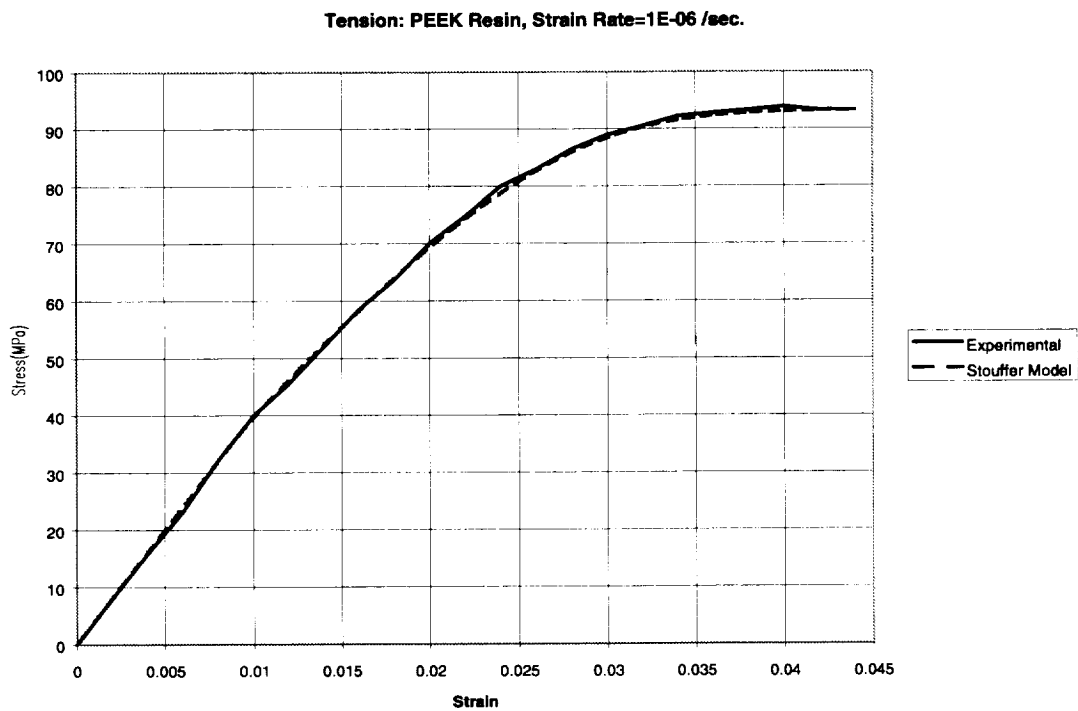


Figure 11: Model Correlations for PEEK at Tensile Strain Rate of 1E-06 /sec.

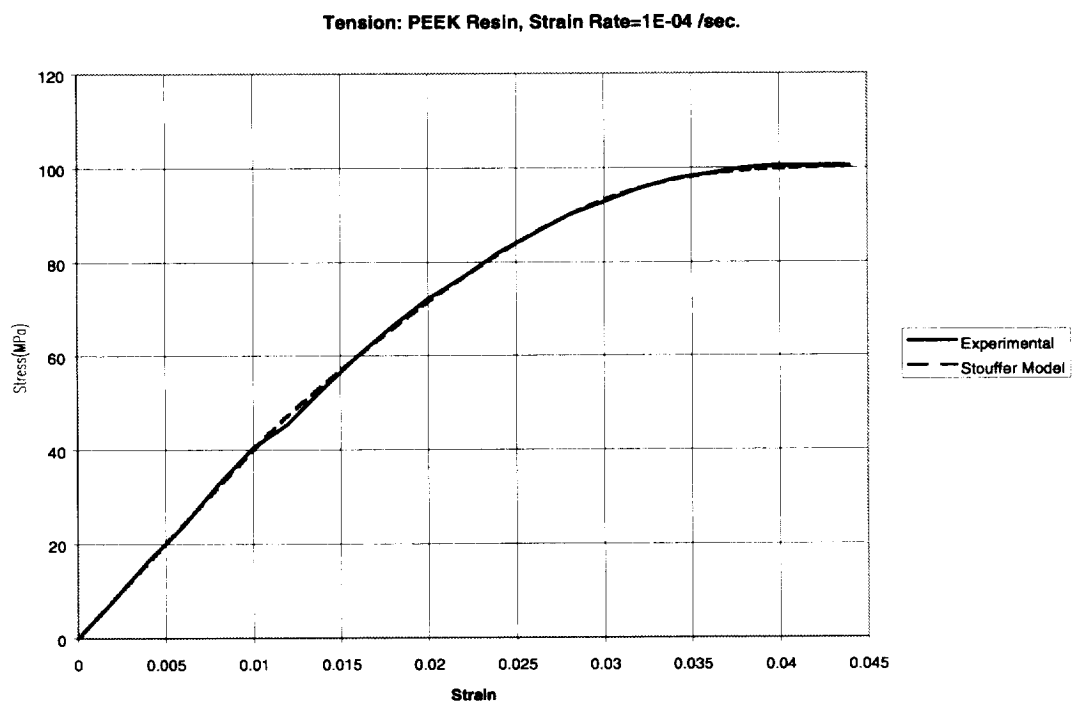


Figure 12: Model Correlations for PEEK at Tensile Strain Rate of 1E-04 /sec.

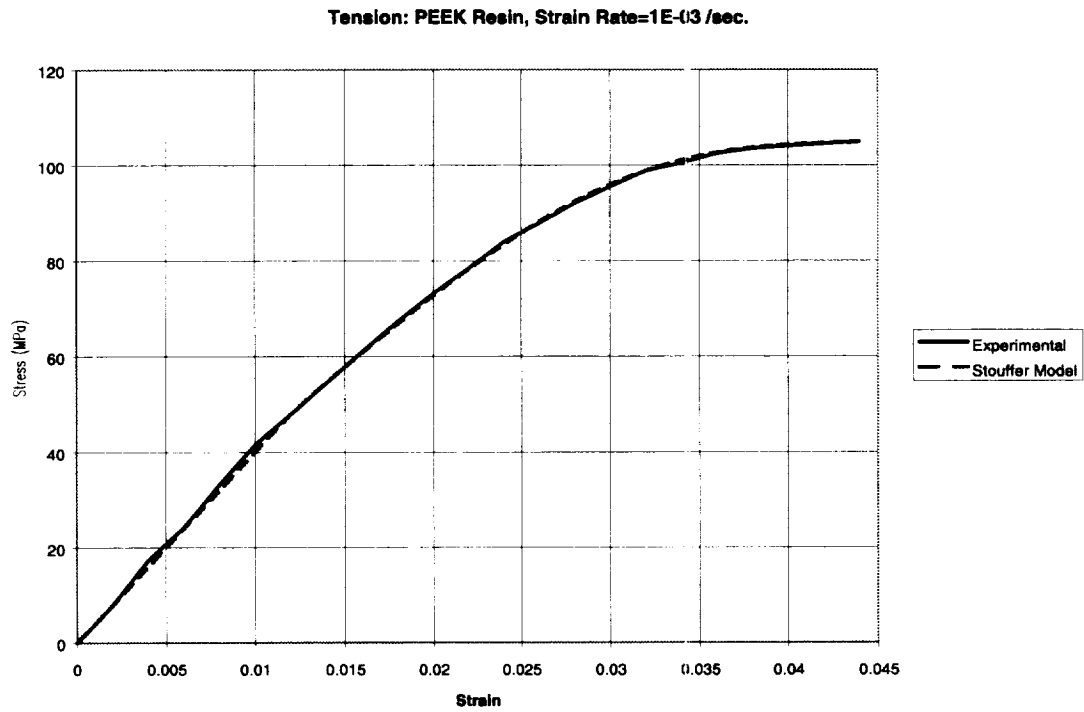


Figure 13: Model Correlations for PEEK at Tensile Strain Rate of 1E-03 /sec.

REPORT DOCUMENTATION PAGE			Form Approved OMB No. 0704-0188	
Public reporting burden for this collection of information is estimated to average 1 hour per response, including the time for reviewing instructions, searching existing data sources, gathering and maintaining the data needed, and completing and reviewing the collection of information. Send comments regarding this burden estimate or any other aspect of this collection of information, including suggestions for reducing this burden, to Washington Headquarters Services, Directorate for Information Operations and Reports, 1215 Jefferson Davis Highway, Suite 1204, Arlington, VA 22202-4302, and to the Office of Management and Budget, Paperwork Reduction Project (0704-0188), Washington, DC 20503.				
1. AGENCY USE ONLY (Leave blank)		2. REPORT DATE August 1998	3. REPORT TYPE AND DATES COVERED Technical Memorandum	
4. TITLE AND SUBTITLE High Strain Rate Deformation Modeling of a Polymer Matrix Composite Part I—Matrix Constitutive Equations			5. FUNDING NUMBERS WU-523-24-13-00	
6. AUTHOR(S) Robert K. Goldberg and Donald C. Stouffer				
7. PERFORMING ORGANIZATION NAME(S) AND ADDRESS(ES) National Aeronautics and Space Administration Lewis Research Center Cleveland, Ohio 44135-3191			8. PERFORMING ORGANIZATION REPORT NUMBER E-11122	
9. SPONSORING/MONITORING AGENCY NAME(S) AND ADDRESS(ES) National Aeronautics and Space Administration Washington, DC 20546-0001			10. SPONSORING/MONITORING AGENCY REPORT NUMBER NASA TM-1998-206969	
11. SUPPLEMENTARY NOTES Robert K. Goldberg, NASA Lewis Research Center, and Donald C. Stouffer, University of Cincinnati, Cincinnati, Ohio 45221. Responsible person, Robert K. Goldberg, organization code 5920, (216) 433-3330.				
12a. DISTRIBUTION/AVAILABILITY STATEMENT Unclassified - Unlimited Subject Category: 24 This publication is available from the NASA Center for AeroSpace Information, (301) 621-0390.			12b. DISTRIBUTION CODE	
13. ABSTRACT (Maximum 200 words) Recently applications have exposed polymer matrix composite materials to very high strain rate loading conditions, requiring an ability to understand and predict the material behavior under these extreme conditions. In this first paper of a two part report, background information is presented, along with the constitutive equations which will be used to model the rate dependent nonlinear deformation response of the polymer matrix. Strain rate dependent inelastic constitutive models which were originally developed to model the viscoplastic deformation of metals have been adapted to model the nonlinear viscoelastic deformation of polymers. The modified equations were correlated by analyzing the tensile/compressive response of both 977-2 toughened epoxy matrix and PEEK thermoplastic matrix over a variety of strain rates. For the cases examined, the modified constitutive equations appear to do an adequate job of modeling the polymer deformation response. A second follow-up paper will describe the implementation of the polymer deformation model into a composite micromechanical model, to allow for the modeling of the nonlinear, rate dependent deformation response of polymer matrix composites.				
14. SUBJECT TERMS Composite materials; Constitutive equations; Strain rate; Viscoplasticity; Viscoelasticity; Impact			15. NUMBER OF PAGES 40	
			16. PRICE CODE A03	
17. SECURITY CLASSIFICATION OF REPORT Unclassified	18. SECURITY CLASSIFICATION OF THIS PAGE Unclassified	19. SECURITY CLASSIFICATION OF ABSTRACT Unclassified	20. LIMITATION OF ABSTRACT	

